Journal of Electroanalytical Chemistry 777 (2016) 33–39

Contents lists available at ScienceDirect

Journal of Electroanalytical Chemistry

journal homepage: www.elsevier.com/locate/jelechem

Prussian blue for electrochromic devices

L.M.N. Assis [a], R. Leones [b], J. Kanicki [c], A. Pawlicka [a,c], M.M. Silva [b,*]

[a] IQSC, Universidade de São Paulo, São Carlos, 13566-590, SP, Brazil
[b] Centro de Química, Universidade do Minho, Gualtar, 4710-057 Braga, Portugal
[c] EECS-University of Michigan, Ann Arbor, MI 48109, USA

ARTICLE INFO

Article history:
Received 12 January 2016
Received in revised form 5 May 2016
Accepted 6 May 2016
Available online 8 May 2016

Keywords:
Prussian blue
DNA- and agar-electrolyte membrane
Electrochromic device

ABSTRACT

All solid electrochromic devices (ECDs) were prepared using Prussian blue (PB) as electrochromic layer, CeO_2-TiO_2 as counter electrode, and either DNA-$Er(CF_3SO_3)_3$ or Agar-$Eu(CF_3SO_3)_3$ as ionic conductive membrane. The ECDs were assembled by combining the natural macromolecule-based electrolyte membrane placed between the glass-ITO/PB and CeO_2-TiO_2/ITO-glass electrodes. The two kind of electrochromic devices were characterized electrochemically and spectroscopically. The electrochemical measurements revealed that applying potentials of −3.0 and +2.0 V promoted the color change of the ECD from blue to transparent. The highest contrast of $\Delta T_{VIS} = 25 \pm 2\%$ was at 686 nm after 60 s of applied potential for ECD with DNA-Er^{3+}-based electrolyte. This ECD showed the charge density of -5.1 mC cm^{-2} after 15 s and -10.4 mC cm^{-2} after 60 s of potential application. Although a successive chronoamperometric (CA) cycling showed the insertion/extraction processes uniform, the ΔT_{VIS} and charge density values dropped down to 5% and -1.6 mC cm^{-2} after 1000 CA cycles, respectively. The ECD with Agar-Eu^{3+}-based electrolyte displayed almost the same charge density values of -5.1 mC cm^{-2} after 15 s and -10.5 mC cm^{-2} after 60 s of −3.0 V potential application. This value decreased to -1.1 mC cm^{-2} after 1400 CA cycles. The best result of ΔT_{VIS} was of $35 \pm 2\%$ at $\lambda = 686$ nm. All the presented results suggest the possibility of using PB as electrochromic coating and natural macromolecules as solid electrolyte in new ECDs development.

1. Introduction

Electrochromic (EC) materials are very interesting because they change their color in a persistent but reversible way due to an electrochemical reaction [1]. This optical change is induced by a small electric current at low DC potentials in the range from a fraction of a volt to a few volts [2,3]. The EC inorganic materials are in general oxides divided in two groups. The first group consists of the materials that change the color under ions insertion, and are named cathodic ECs. The second group consists of materials that change the color during ions extraction, and consequently, they are named anodic ECs. In the last years, many transition metal oxides such as W, Ir, Mn, and Co have been studied for their electrochromic properties, and for their major stability when compared to the organic electrochromic compounds. WO_3 is one of the first studied electrochromic oxides. Usually, it is obtained by synthesis methods that vary from electrochemical [2], sol-gel [4], pulsed laser deposition techniques [5] to sputtering [6,7]. In the last five years, the number of published papers on EC materials has doubled confirming the great interest of the scientific community on this subject. The main reason for that is a possibility to develop new and modern devices such as electrochromic.

Different EC devices (ECDs) are today in the market with niche products in automotive, building windows, and displays sectors. For automotive industry, Gentex and Donnelly in the USA are producing auto dimming rear mirrors [8]. For display industry, NTERA is producing iPod EC displays [9,10]. Unfortunately, these devices present several disadvantages such as the use of expensive deposition processes, the application of high flammable and low stability liquid electrolytes (e.g. PC-$LiClO_4$), and the long switching times of the devices. The application of EC devices for thermal management for instance is limited to the Ferrari Superamerica roof panel [11]; nevertheless, its cost is extremely high. To overcome problems above, it is necessary to develop new electrochromic devices that will be less expensive and can be applied with success in several light transmitting and/or reflecting products [12].

Electroactive layers compose all solid-state ECDs, and electrochromic materials are separate from counter electrode by polymer electrolyte. Prussian blue (PB) is a well-known EC material that changes the color from blue to transparent [13]. The two forms of PB are called insoluble $Fe^{III}_4[Fe^{II}(CN)_6]_3$ and the soluble $MFe^{III}Fe^{II}(CN)_6$, where M is an alkaline metal. The simple method to obtain the PB is by electrodeposition [14]. The nature of the counter electrode will have direct impact on ECD properties [1,15]. As already shown in several publications, CeO_2-TiO_2 is a good counter electrode thin film. It can reversibly undergo redox reactions without changing the color. It can be also obtained by simple sol-gel method coupled to dip-coating technique deposition [16].

* Corresponding author.
E-mail address: nini@quimica.uminho.pt (M.M. Silva).

http://dx.doi.org/10.1016/j.jelechem.2016.05.007
1572-6657/

Aiming to develop new all solid-state ECDs windows with glass/ITO/PB/electrolyte membrane/CeO_2–TiO_2/ITO/glass configuration were assembled and characterized by electrochemical and spectroscopic methods.

2. Experimental section

2.1. Polymer electrolyte membrane preparation

The polymer electrolytes membrane were synthesized according to the method described by Leones et al. [17]. Salmon sperm-DNA (0.5 g, Ogata Research Laboratory, Japan) was dispersed in 20 mL of Milli-Q® water, and heated under magnetic stirring up to 60 °C for a few minutes for complete dissolution. To this solution were added different quantities of erbium triflate ($Er(CF_3SO_3)_3$) [18] and glycerol (Himedia, 99.5%) as plasticizer.

The polymer electrolytes membrane were synthesized according to the method described by Raphael et al. [19]. Samples of $Agar_nEu(CF_3SO_3)_3$ were prepared by dissolving 0.5 g of agar (Sigma-Aldrich) in 30 mL of Milli-Q® water under heating up to 100 °C and magnetic stirring for a few minutes for complete dissolution. 0.5 g of glycerol (Himedia, 99.5% of purity) acting as plasticizer and $Eu(CF_3SO_3)_3$ (Sigma Aldrich, 98% of purity) were added to this solution under stirring.

The resulting solutions were poured on Petri dishes, cooled at room temperature, and then dried in a Büchi oven at 60 °C for 8 to 12 days to form transparent membranes of about 0.9 mm of thickness [20,21].

2.2. Glass/ITO/Prussian blue and glass/ITO/CeO_2-TiO_2 electrodes preparation

Prussian blue (PB) films with thickness of about 217 nm [22] where electrodeposited from a solution containing 5 mL of HCl (0.05 mol L^{-1}), 10 mL of $K_3Fe(CN)_6$ (0.05 mol L^{-1}), and 10 mL of $FeCl_3 \cdot 6H_2O$ (0.05 mol L^{-1}) over glass/ITO (Delta Technologies; CG-50IN-1507; 8–12 Ω) substrates; this was a working electrode. One square centimeter platinum plate as counter electrode and Ag/AgCl as reference electrode were used. A cathodic current density of −40 μA cm^{-2} was applied for 300 s with an Autolab 302N on between ITO and Pt promoting a deposition of the Prussian blue coating. Next, the glass/ITO/PB was removed from the solution and washed with Milli-Q® water.

The CeO_2–TiO_2 thin films were deposited from sol–gel solution over glass/ITO substrate. The dip-coating method was used with the withdrawal rate of 20 cm min^{-1} and final annealing temperature of 450 °C for 15 min, as described previously [16].

2.3. ECD cell assembly

The electrochromic devices (ECDs) with one square centimeter area and having the configuration glass/ITO/PB/electrolyte membrane/CeO_2–TiO_2/ITO/glass were assembled. Two electrodes previously prepared faced each other and were separated by polymer electrolyte membrane of thickness of 0.9 mm. The thickness of the electrolyte controlled the cell thickness. Electrical contacts were applied to ITO surface. Aiming to improve this contact a one cm wide Cu-conducting tape (3 M) was glued to the ITO. The edges of the mounted cells were sealed with a protective and insulating tape (3 M).

2.4. Measurements

The electrochemical measurements of ECDs were performed with an Autolab 302N apparatus. The cyclic voltammetries were registered during applied potentials ranging from −3.0 to +2.0 V with the electric field scan step of 100 mV s^{-1}. The chronoamperometric (CA) measurements were done using a square wave of −3.0 and +2.0 V for 15, 30, and 60 s each. It means that one CA cycle was composed of application of −3.0 V for 60 s and +2.0 V for next 60 s (Fig. 2a). The same procedure was used for 15 and 30 s of applied potentials.

The UV–vis spectroscopy measurements of electrochemical cell were recorded with an Agilent 8453 between 200 and 1100 nm after application of −3.0 and +2.0 V for 15, 30, and 60 s.

3. Results and discussion

3.1. ECD with the DNA-Er^{3+}

The voltammograms for ECD were registered between −3.0 and +2.0 V at a scan rate of 100 mV s^{-1}, and a representative curve is displayed in Fig. 1. It is possible to observe in this figure that the application of an increasingly negative voltage to the ECD in the dark blue color state leads to an increase in the cathodic current, and it is accompanied by a simultaneous change to bleached state (transparent). Three peaks are observed in the voltammogram instead of four peaks characteristic to the PB [23]. Two cathodic peaks at −0.8 and 0.9 V and one anodic peak at 1.0 V are observed and can be attributed to PW, PB, and PG, respectively. The anodic peak was responsible for the blue coloring of the PB and the ECD. From this figure, it seems that the reactions described in Eqs. (1) and (2) [23,24] that are ascribed to PW to soluble PB and PG to PB transitions, respectively are not very clear in ECD voltammogram; consequently, peak at 1.0 V can be either of PG or insoluble PB shifted to more positive potential. The shape of ECD voltammogram in Fig. 1 is probably due to electrolyte composition, where no additional potassium and iron ions are present, rather than to the PB film. Finally, the redox processes seem to be not fully reversible [25].

$$\underset{\text{Waterinsoluble PB}}{Fe_4^{3+}\left[Fe^{2+}(CN)_6\right]_3} + 4K^+ + 4e^- \iff \underset{\text{Everitt's salt (PW)}}{K_4Fe_4^{2+}\left[Fe^{2+}(CN)_6\right]_3} \quad (1)$$

$$\underset{\text{Waterinsoluble PB}}{Fe_4^{3+}\left[Fe^{2+}(CN)_6\right]_3} - 3e^- + 3A^- \iff \underset{\text{Prussiangreen (PG)}}{Fe_4^{3+}\left[Fe^{3+}(CN)_6A^-\right]_3} \quad (2)$$

Aiming to verify the possibility of use of the DNA-erbium triflate as ionic conducting membrane, small ECDs with glass/ITO/PB/DNA-$Er(CF_3SO_3)_3$/CeO_2-TiO_2/ITO/glass configuration were assembled and characterized. The charge density ($Q = \int_0^t Id t$) / A (I-current, t-time, and A-area) responses measured by applying −3.0 V/+2.0 V in the three time intervals of 15, 30, and 60 s of this ECD is shown in Fig. 2a.

From Fig. 2a it can be stated that the insertion of charge (Q_{in}) for 15 s at −3.0 V of applied voltage reached −5.1 mC cm^{-2}, and the inverse potential application of 2.0 V during next 15 s promoted the extraction

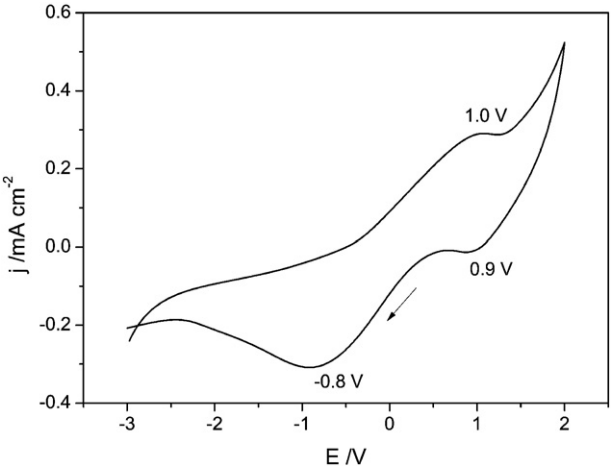

Fig. 1. Cyclic voltammograms at v = 100 mV s^{-1} of the ECD with glass/ITO/PB/DNA-Er^{3+}/CeO_2-TiO_2/ITO/glass configuration after 3rd CA cycle.

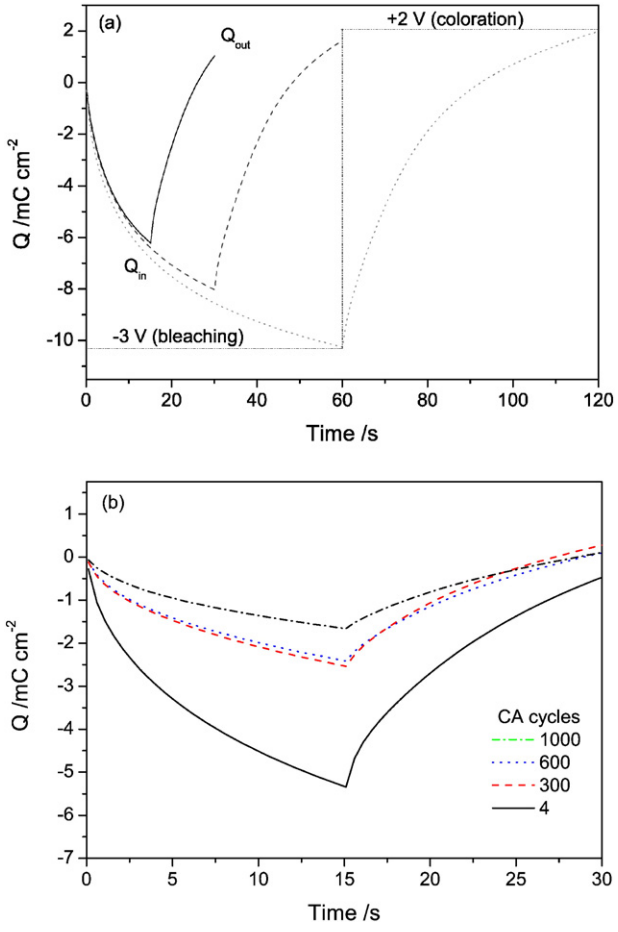

Fig. 2. Charge density of ECD with glass/ITO/PB/DNA-Er^{3+}/CeO_2TiO$_2$/ITO/glass configuration for applied potentials of −3.0 to +2.0 V; (a) 1st cycle for 15 (continues black line), 30 (dashed blue line) and 60 s (dotted red line); square wave of −3.0 and +2.0 V for 60 s each (dash dot dash black line); and (b) chronoamperometric (CA) cycles applied for 15 s; cycle 4 (black continues line), 300 (dashed red line), 600 (dotted blue line) and 1000 (green dash dot dash line).

of charge (Q_{out}). The same potentials applied for 30 and 60 s resulted in a charge density of −7.9 and −10.4 mC cm^{-2} of charge insertion and consequent extraction, respectively. During the first cycle, the ratio of the anodic (Q_{out}) to the cathodic (Q_{in}) charge densities (Q_{out}/Q_{in}; Fig. 2a) is 1.0, denoting an almost completely reversible intercalation/desintercalation process. These obtained values are considerably lower than that reported previously for a glass/ITO/WO_3/electrolyte/ITO/glass ECD with d-PCL(530)/siloxane$_{6.1}$LiCF$_3$SO$_3$Eu(CF$_3$SO$_3$)$_3$ as electrolyte [26] but higher than 1.8 mC cm^{-2} and −2.6 mC cm^{-2} displayed by glass/ITO/WO_3/DNA-LiI/I_2/CeO_2-TiO_2/ITO/glass and glass/ITO/WO_3/DNA1GLY1PB2/CeO_2–TiO_2/ITO/glass ECDs, respectively [27,28].

The redox stability (Q_{out}/Q_{in}) of the ECD was checked through chronoamperometric (CA) cycling by applying potential steps of −3.0 V/+2.0 V for 15 s intervals during 300, 600, and 1000 cycles (Fig. 2b). The CA data obtained for the 4th, 300th, 600th, and 1000th cycle are reproduced in Fig. 2b. During insertion/extraction cycling, the PB insoluble form is fully reversible converted to the soluble form [29], but this conversion probably is not fully quantitative [30]. Consequently, after reductive cycling the electroactive films present a composition intermediate between the soluble and insoluble form. The results displayed in Fig. 2b also demonstrate the insertion and extraction in ECD cell is almost fully reversible. In addition, we can say that during the first cycles there are more inserted/extracted charges than during the subsequent cycles (Table 1). The coloration of the devices is a result of anodic process, and comparing the first 2 s of cathodic and anodic processes (Table 1) it can be stated that bleaching (Q_{in}) is slightly faster than coloring (Q_{out}) [25]. Therefore, these findings corroborate with other results already published as for example for the ECD with glass/ITO/WO_3/d-PCL(530)/siloxane$_{5.2}$LiCF$_3$SO$_3$Eu(CF$_3$SO$_3$)$_3$/ITO/glass configuration, where the bleaching kinetics was faster than the coloration one [26]. However, as observed in Table 1, after 15 s of applied potential the values of Q_{out} are higher than the values of Q_{in}, what means that more charges remain in anodic process than in cathodic one. Fig. 2b shows also that after 1000 CA cycles the value of the Q_{in} decreased from −5.1 to −1.6 mC cm^{-2}. This decrease can be attributed to the loss of Fe^{3+} high spin during the redox reaction between the insoluble and soluble PB, and by not fully reversible insertion and extraction of charge [25]. These results indicate that there is degradation of ECD with the increasing number of CA cycling. Finally, the Q_{out}/Q_{in} changes with CA cycles number, and it is associated with the ECD degradation over time.

For the determination of transmittance and absorbance differences (ΔT_{VIS} and ΔOD_{VIS}) of the glass/ITO/PB/DNA-Er^{3+}/CeO_2-TiO_2/ITO/glass device the UV–vis spectra were obtained in the bleached (transparent) and blue colored states after the application of −3.0 and +2.0 V during 60 s, respectively. The transmittance spectra recorded during the 1st cycle are depicted in Fig. 3.

As one can see in Fig. 3 there was a difference in the UV–vis-NIR spectra values between colored and bleached states of device. During positive potential application, i.e., coloration and/or oxidation the ECD changed from transparent Prussian white (PW, Everitt's salt) to dark blue Prussian blue (PB). The inverse process of bleaching occurred during a reduction of PB [25]. The highest difference was observed in the 600 to 800 nm range. The values of the ΔT_{VIS} at 633 and 686 nm for 15, 30, and 60 s of potential application are listed in Table 2. As in other ECDs also in this one, the longer times of charge insertion promoted deeper coloration. The best result of $\Delta T_{VIS} = 25 \pm 2\%$ was at 686 nm for 60 s of applied potential, where the ECD switched between $T_{colored} = 8\%$ and $T_{bleached} = 33\%$ values. The 25% color change value is significantly higher than $\Delta T = 3.5\%$ reported for ECD with glass/ITO/WO_3/DNA-LiI/I_2/CeO_2-TiO_2/glass [27] or $\Delta T = 7\%$ for ECD with glass/ITO/WO_3/DNA$_n$Er(CF$_3$SO$_3$)$_3$)/CeO_2-TiO_2/ITO/glass configuration [20]. The differences can be due to the electrochromic coating or lithium salt used in the electrolyte.

The reversibility and stability of the ECD were studied by chronoamperometric cycling coupled to UV–vis spectroscopic measurements. Fig. 4 shows the time dependence of the transmittance of the glass/ITO/PB/DNA-Er^{3+}/CeO_2-TiO_2/ITO/glass ECD with potential steps of −3.0 V/+2.0 V at every 15 s for 1000 cycles. It is observed that after 1000 cycles the window with configuration glass-ITO/PB/DNA-Er^{3+}/CeO_2-TiO_2/ITO-glass is reversible and features $\Delta T = 5\%$ at λ = 686 nm. This value is lower than $\Delta T = 18\%$ after 5000 cycles found in literature [31]. The subsequent insertion and extraction of charges is responsible for a decrease of transmittance variation between colored and bleached states. After 1000 cycles the dark color state of the device becomes less intense color, and the transparent state becomes light blue color.

Table 1
Charge values at 2 and 15 s of bleached (Q_{in}) and colored (Q_{out}) states of ECD with configuration glass/ITO/PB/DNA-Er^{3+}/CeO_2TiO$_2$/ITO/glass for 1, 300, 600, and 1000th chronoamperometric (CA) cycle.

CA cycle	$-Q_{in}$/mC cm^{-2}		$-Q_{out}$/mC cm^{-2}		Q_{out}/Q_{in}
	2/s	15/s	2/s	15/s	15/s/15/s
4	1.9	5.1	1.5	4.9	1.0
300	0.8	2.4	0.8	2.6	1.1
600	0.8	2.3	0.6	2.3	1.0
1000	0.6	1.6	0.4	1.8	1.1

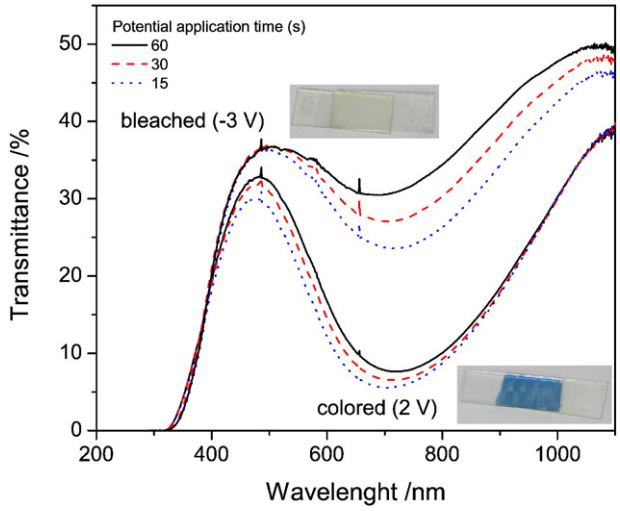

Fig. 3. Transmittance for the colored and bleached states of ECD with glass/ITO/PB/DNA-Er^{3+}/CeO_2TiO_2/ITO/glass configuration for applied potentials of −3.0 to +2.0 V, for 60 s (continues lines), 30 s (dashed lines), and 15 s (dotted lines). A selected picture shows the appearance of the ECD composed of DNA based Er^{3+} in the colored and bleached states.

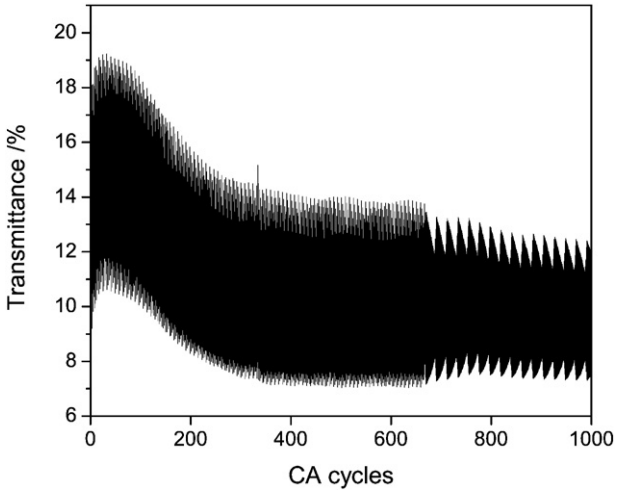

Fig. 4. Transmittance at λ = 686 nm in function of the chronoamperometric (CA) cycles of insertion and extraction of charges for ECD with glass/ITO/PB/DNA-Er^{3+}/CeO_2TiO_2/ITO/glass configuration. Applied potential of −3.0 V/+2.0 V during 15 s/15 s.

3.2. ECD with the Agar-Eu^{3+}

The ECD with glass-ITO/PB/$Agar_nEu(CF_3SO_3)_3$/CeO_2-TiO_2/ITO-glass configuration was examined by CV, and the voltammograms were registered between −2.8 and 1.5 V at a scan rate of 100 mV s^{-1} (Fig. 5). The voltammogram of the 3rd cycle showed two cathodic peaks at −0.5 and 1.0 V. Analysing Fig. 6 it can be stated that the voltammogram is similar to the one registered for device with glass-ITO/PB/DNA-Er^{3+}/CeO_2-TiO_2/ITO-glass configuration; however, both cathodic and one anodic peaks were registered at different potentials. In this case the negative cathodic peak is shifted to more positive value of −0.5 V and anodic peak is shifted to more negative value, i.e., to 0.2 V, suggesting that both peaks form a redox pair attributed to the conversion of Prussian white (Everitt's salt) to Prussian blue (Eq. (1)). Consequently, no PG peak is observed. As the configuration of both devices is the same except the electrolyte, where one was based on DNA-Er^{3+} and other on Agar-Eu^{3+}this difference can be attributed to the electrolyte rather than to the PB film. Furthermore, the shape of voltammogram differs from that found for the device with glass-ITO/WO_3/Agar-based electrolyte/CeO_2-TiO_2/ITO-glass configuration, where cathodic peak was centered in the range of −0.7 to −1.1 V, depending on the sample [32]. The anodic electrochemical response of the ECDs with Agar-$LiClO_4$ and Agar-$Eu(pic)_3$ membranes was composed by two peaks, where one was large and its maximum was centered in between −0.3 and −0.03 V. The second one was small and centered in between 0.4 and 0.7 V. The presence of this additional oxidation process was probably due to the electrolyte as already observed for ECDs composed of WO_3/gelatin-glycerol/CeO_2-TiO_2 [33] but different of ECD composed of WO_3/starch-glycerol/CeO_2-TiO_2 [13].

Table 2
Transmittance difference values measured between colored and bleached states at 633 and 686 nm for ECD with glass/ITO/PB/DNA-Er^{3+}/CeO_2TiO_2/ITO/glass configuration after coloring and bleaching for 15, 30, and 60 s.

λ/nm	ΔT/%		
	15/s	30/s	60/s
633	15	19	23
686	16	20	25

The charge density response measured by chronoamperometry at −3.0 V/+2.0 V; 15 s/15 s, 30 s/30 s, and 60 s/60 s steps of ECD containing solid electrolyte based on agar and $Eu(CF_3SO_3)_3$ is shown in Fig. 6a. The result showed an increase of charge density (Q_{in}) with time reaching −5.2 mC cm^{-2} when the potential of −3.0 V was applied for 15 s. The same applied potential for 30 to 60 s resulted in Q_{in} of −7.2 and −10.5 mC cm^{-2}, respectively. These values are higher than found by Leones et al. [34] for the device with glass/ITO/WO_3/Agar-[C_2mim][C_2SO_4]/CeO_2-TiO_2/ITO/glass configuration. The difference can be due to the ionic liquid that was used in the electrolyte composition. Moreover, the anodic (Q_{out}) to the cathodic (Q_{in}) charge densities ratio (Q_{out}/Q_{in}) obtained for the ECD studied here was 1.0 denoting an almost completely reversible process.

The charge density responses measured by chronoamperometry for the cycles 4, 100, 200, 400, and 1400 are shown in Fig. 6b. The results displayed in this figure show that again during the first CA cycles there is more inserted/extracted charges than during the subsequent cycles. It is also noticed that the initial charge at t = 0 s is slightly different from charge value at the end of the cycle at t = 30 s. A consecutive CA cycling of the devices leads to the decrease of inserted and extracted charges. Moreover, differently of the ECD with DNA-Er^{3+} electrolyte this ECD shows that the charges of bleaching (Q_{in}) are slightly lower than of coloring (Q_{out}) in the first 2 s and after 15 s of cathodic and anodic processes (Table 3). From these measurements, it can be stated that

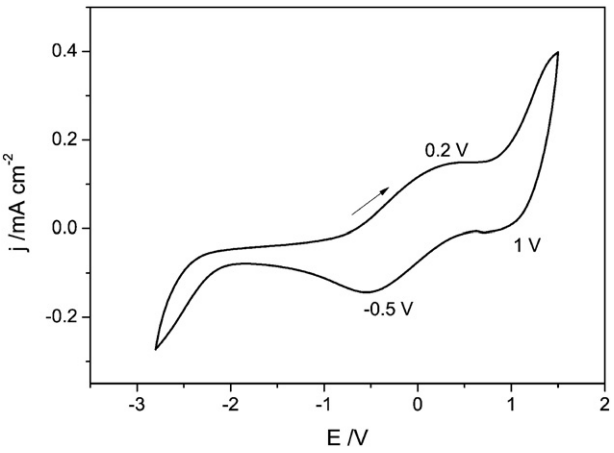

Fig. 5. Cyclic voltammogram of the ECD with glass/ITO/PB/Agar-Eu^{3+}/CeO_2TiO_2/ITO/glass configuration registered at v = 100 mV s^{-1} after 3rd CA cycle.

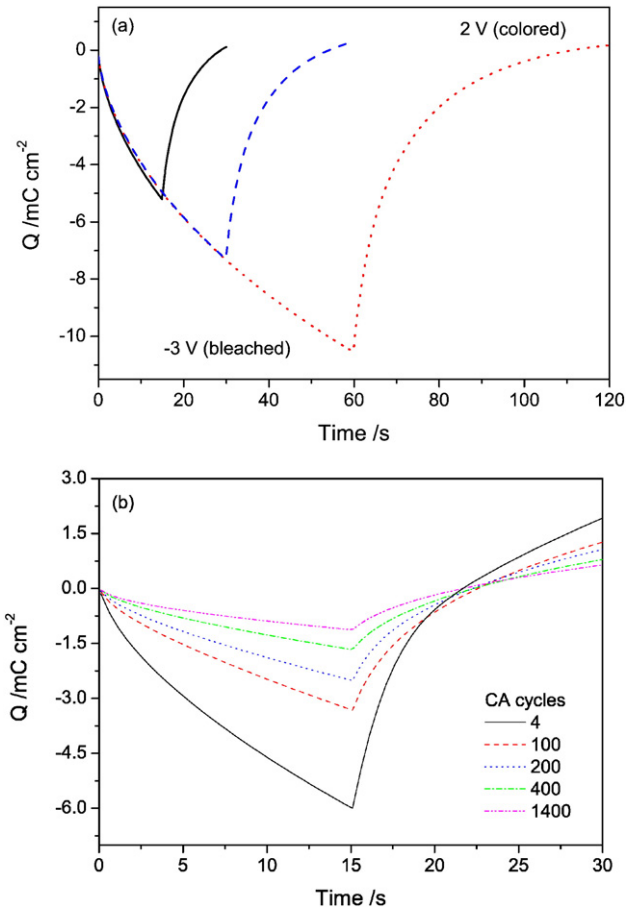

Fig. 6. Charge density of ECD with glass-ITO/PB/Agar-Eu^{3+}/CeO_2-TiO_2/ITO-glass configuration for applied potentials of −3.0 to +2.0 V; (a) 1st cycle for applied potentials for 15, 30, and 60 s and (b) chronoamperometric (CA) cycle applied for 15 s; cycle 4 (black continues line), 100 (dashed red line), 200 (dotted blue line), 400 (dash dot dash green line), and 1400 (dash dot dot dash pink line).

the increase of chronoamperometric cycling is leading to a decrease of the inserted charge values reaching −1.1 mC cm^{-2} for the 1400 cycle (Fig. 6b). Table 3 reveals also an increase of Q_{out}/Q_{in} values with CA cycling of the ECD. The decrease of Q_{in} charges and the increase of Q_{out}/Q_{in} values are most likely due to ECD degradation over time. However, the charge density values of this ECD are comparable to the results discussed above as well as to −4.8 mC cm^{-2} shown by Costa et al. [35] for the device with a glass-ITO/WO_3/starch-Li(ClO_4)/CeO_2-TiO_2/ITO-glass or to the ECD with agar-based electrolyte [33]. This would indicate that the process is not fully reversible.

Fig. 7 shows the device transmittance spectra with glass-ITO/PB/Agar-Eu^{3+}/CeO_2-TiO_2/ITO-glass configuration. The figure depicts the variation in transmittance depending on the wavelength with different

Table 3
Charge values at 2 and 15 s of bleached (Q_{in}) and colored (Q_{out}) states of ECD with configuration glass/ITO/PB/DNA-Er^{3+}/CeO_2TiO_2/ITO/glass for 1, 100, 200, 400, and 1400th chronoamperometric (CA) cycle.

CA cycle	$-Q_{in}$/mC cm^{-2}		$-Q_{out}$/mC cm^{-2}		Q_{out}/Q_{in}
	2/s	15/s	2/s	15/s	15/s/15/s
4	1.5	5.9	3.4	7.9	1.3
100	0.8	3.3	1.5	4.6	1.4
200	0.7	2.5	1.2	3.6	1.4
400	0.5	1.7	0.8	2.5	1.5
1400	0.4	1.1	0.5	1.7	1.5

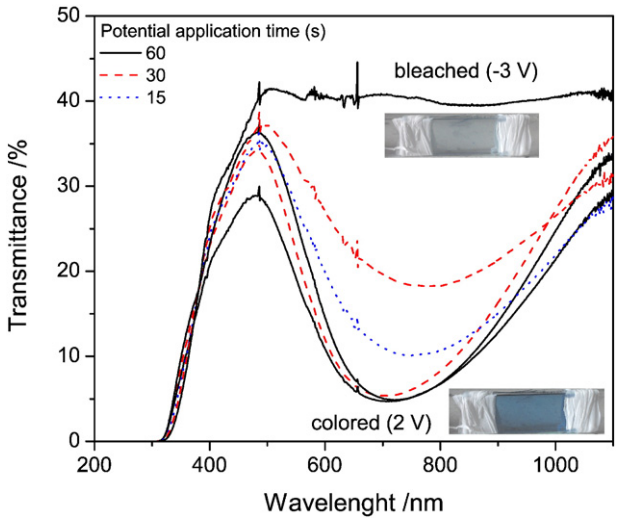

Fig. 7. Transmittance of ECD with glass/ITO/PB/Agar-Eu^{3+}/CeO_2TiO_2/ITO/glass configuration for applied potentials of −3.0 to +2.0 V, for 60 s (continues lines), 30 s (dashed lines), and 15 s (dotted lines). A selected pictures show the appearance of the ECD composed of Agar based Eu^{3+} in the colored and bleached states.

loading times of insertion and extraction. The values of the ΔT_{VIS} at 633 and 686 nm for 15, 30, and 60 s of potential application are listed in Table 4. As in the previous ECD also in this one the longer times of charge insertion promoted deeper coloration.The best result of $\Delta T = 35 \pm 2\%$ at $\lambda = 686$ nm was obtained by applying potentials of −3.0 and 2.0 V for 60 s. This result was lower than $\Delta T = 48\%$ at 550 nm found on devices with WO_3/agar-CH_3COOH/CeO_2-TiO_2 configuration [32].

Fig. 8 shows the time dependence of the transmittance of the glass/ITO/PB/Agar-Eu^{3+}/CeO_2-TiO_2/ITO/glass ECD with potential steps of −3.0 V/+2.0 V at every 15 s during 1483 cycles. As one can see in this figure the transmittance difference of the device during the consecutive color/bleaching cycling up to 300 CA cycles is about 8% switching between 5 and 13%. At 500 CA cycles the transmittance value of the colored state decreases to 4% and after that slightly increases. As can be seen in this Fig. 8, the color/bleaching difference oscillates between 4 and 5% up to 1483 cycles. At the end of this experiment, the colored state of the device is replaced by a less intense color, and the transparent state is replaced by a light blue color.

3.3. Application of ECDs

Prussian Blue electrochromic properties are due to change from a blue color (PB) to color-less (PW), which is characterized by mixed valence forms of Fe^{3+}/Fe^{2+} and Fe^{2+}/Fe^{2+}, respectively. Giménez-Romero et al. [36] have shown that this PB ⟺ PW electron transfer occurs by means of different processes in different ionic sites inside the Prussian blue crystalline structure. One of them corresponds to the oxidation of low spin Fe^{2+} to high spin Fe^{3+}-CN units that are close to potassium cations, which serve to exchange the electrical charge. The second one is associated to the oxidation of low spin Fe^{3+} to high spin

Table 4
Transmittance difference values measured between colored and bleached states at 633 and 686 nm for ECD with PB/Agar-Eu^{3+}/CeO_2-TiO_2 configuration after coloring and bleaching for 15, 30, and 60 s.

λ/nm	ΔT/%		
	15/s	30/s	60/s
633	6.2	15.4	32.4
686	6.3	16.8	35.2

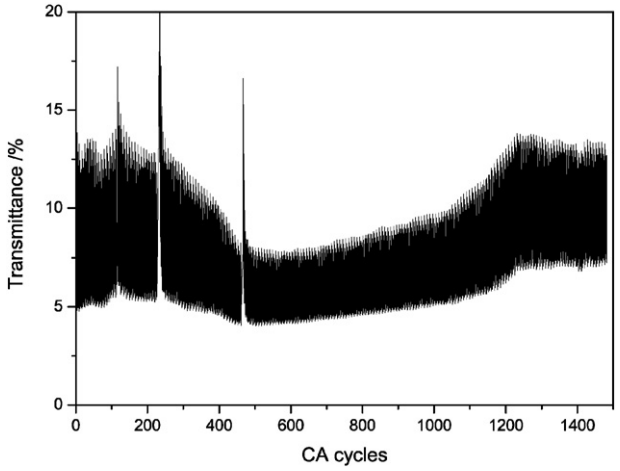

Fig. 8. Transmittance at λ = 686 nm in function of the chronoamperometric (CA) cycles of insertion and extraction of charges of the glass/ITO/PB/Agar-Eu^{3+}/CeO_2-TiO_2/ITO/glass configuration during 1483 color/bleaching cycles under application of −3.0 V/+2.0 V for 15 s each.

Fe^{2+}-CN trapped sites, and the third one is similar to the first one, i.e., oxidation of low spin Fe^{2+} to high spin Fe^{3+}-CN units, far from potassium cations and balanced by electrical charge exchanged with anions [37].

From our results, we can conclude that ECD will allow modulating visible light transmission. The light modulation could lead to different application. Some of the ECDs devices are already used as rearview mirrors in modern cars, and they provide glare attenuation during night driving [38]. The same purpose for small aircraft windows dimming was also envisaged [8]. Although, some few practical applications in architecture can be found over the world [39], the challenge to find better solutions continue [12,40]. Finally, it was already shown that ECDs have potential to save lighting energy when compared to ordinary clear glass [41], so they are interesting systems to be studied.

4. Conclusions

The Prussian blue films were applied in small ECDs with glass-ITO/PB/DNA-Er$(CF_3SO_3)_3$-electrolyte/CeO_2-TiO_2/ITO-glass and glass-ITO/PB/Agar-Eu$(CF_3SO_3)_3$-electrolyte/CeO_2-TiO_2/ITO-glass configurations. The ECDs' color change between blue and bleached states depended on the potential pulse duration being the best result of $\Delta T_{VIS} = 25 \pm 2\%$ at 686 nm after 60 s/60 s of applied potential for ECD with DNA-Er^{3+}-based electrolyte. This ECD showed the charge density of -5.3 mC cm^{-2} after 15 s and -10.4 mC cm^{-2} after 60 s of potential application. Although, a successive chronoamperometric (CA) cycling showed the insertion/extraction processes uniform, the ΔT_{VIS} and charge density values dropped down to 5% and -1.6 mC cm^{-2} after 1000 CA cycles, respectively. The ECD with Agar-Eu^{3+}-based electrolyte displayed almost the same charge density values of -5.2 mC cm^{-2} after 15 s and -10.5 mC cm^{-2} after 60 s of -3.0 V potential applications. This value decreased to -1.1 mC cm^{-2} after 1483 CA cycles. The best result of ΔT_{VIS} was of $35 \pm 2\%$ at λ = 686 nm. All the presented results suggest that the investigated ECD present good performance/properties and can be a promising solution for display applications.

Acknowledgments

The authors are indebted to Fundação para a Ciência e Tecnologia (Portugal) for FEDER (PEst-C/QUI/UI0686/2013) and SFRH/BD/90366/2012 grant (R. Leones), FAPESP (grant 2012/14103-3), CNPq/STATOIL (grant 201820/2014-5), CAPES (grant 2765/2010), and European Community for FP7-PEOPLE-2009-IRSES Biomolec – 247544 for the financial support given to this research. M. M. Silva acknowledges CNPq (PVE grant 406617/2013-9) for the mobility grant provided by this institution.

References

[1] P.M.S. Monk, R.J. Mortimer, D.R. Rosseinsky, Electrochromism and Electrochromic Devices, Cambridge University Press, New York, 2007.
[2] M. Deepa, M. Kar, D.P. Singh, A.K. Srivastava, S. Ahmad, Influence of polyethylene glycol template on microstructure and electrochromic properties of tungsten oxide, Sol. Energy Mater. Sol. Cells 92 (2008) 170.
[3] C.G. Granqvist, Oxide electrochromics: why, how, and whither, Sol. Energy Mater. Sol. Cells 92 (2008) 203.
[4] S. Heusing, M.A. Aegerter, Sol-gel coatings for electrochromic devices, in: M. Aparicio, A. Jitianu, L.C. Klein (Eds.), Sol-Gel Processing for Conventional and Alternative Energy, 3312, Springer US, Boston, MA 2012, p. 239.
[5] V. Teixeira, H.N. Cui, L.J. Meng, E. Fortunato, R. Martins, Amorphous ITO thin films prepared by DC sputtering for electrochromic applications, Thin Solid Films 420 (2002) 70.
[6] H.N. Cui, V. Teixeira, A. Monteiro, E. Fortunato, R. Martins, E. Bertran, Physical properties of sputtered ITO and WO3 thin films, Materials Science Forum, Trans Tech Publ, vol. 455 2004, p. 7.
[7] A. Georg, A. Georg, W. Graf, V. Wittwer, Switchable windows with tungsten oxide, Vacuum 82 (2008) 730.
[8] Aerospace overview, http://www.gentex.com/aerospace/aerospace-overview (accessed on 11/06/2015).
[9] Digital ink prototype uses nanotech, http://www.extremetech.com/extreme/74496-digital-ink-prototype-uses-nanotech (accessed on 13/03/2015).
[10] Sol-gel electrochromic devices, http://www.solgel.com/articles/Mar02/ntera.asp (accessed on 13/03/2015).
[11] Superamerica, http://auto.ferrari.com/en_US/sports-cars-models/past-models/superamerica/ (accessed on 13/03/2015).
[12] V. Seshadri, J. Padilla, H. Bircan, B. Radmard, R. Draper, M. Wood, T.F. Otero, G.A. Sotzing, Optimization, preparation, and electrical short evaluation for 30 cm^2 active area dual conjugated polymer electrochromic windows, Org. Electron. 8 (2007) 367.
[13] A. Pawlicka, D.C. Dragunski, C.O. Avellaneda, Electrochromic devices with starch based solid polymeric electrolytes, in: A. Graja, B.R. Bulka, F. Kajzar (Eds.), Conference of the NATO Advanced Research Workshop on Molecular Low-dimension and Nanostructured Material for Advanced Applications, vol. 59, Kluwer Academic Publishers, Poznan, Poland 2002, p. 255.
[14] J. Agrisuelas, P.R. Bueno, F.F. Ferreira, C. Gabrielli, J.J. Garcia-Jareno, D. Gimenez-Romero, H. Perrot, F. Vicente, Electronic perspective on the electrochemistry of Prussian blue films, J. Electrochem. Soc. 156 (2009) P74.
[15] E. Masetti, F. Varsano, F. Decker, Sputter-deposited cerium vanadium mixed oxide as counter-electrode for electrochromic devices, Electrochim. Acta 44 (1999) 3117.
[16] C.O. Avellaneda, A. Pawlicka, Preparation of transparent CeO2-TiO2 coatings for electrochromic devices, Thin Solid Films 335 (1998) 245.
[17] R. Leones, L.C. Rodrigues, M. Fernandes, R.A.S. Ferreira, I. Cesarino, A. Pawlicka, L.D. Carlos, V. de Zea Bermudez, M.M. Silva, Electro-optical properties of the DNA-Eu^{3+} bio-membranes, J. Electroanal. Chem. 708 (2013) 116.
[18] A.R. Goncalves, C.J.R. da Silva, M.M. Silva, M.J. Smith, Ionic conduction and thermal properties of poly(ethylene oxide)-Er (CF3SO3)3 films, Ionics 1 (1995) 342.
[19] E. Raphael, C.O. Avellaneda, M.A. Aegerter, M.M. Silva, A. Pawlicka, Agar-based gel electrolyte for electrochromic device application, Mol. Cryst. Liq. Cryst. 554 (2012) 264.
[20] R. Leones, M. Fernandes, F. Sentanin, I. Cesarino, J.F. Lima, V.d.Z. Bermudez, A. Pawlicka, C.J. Magon, J.P. Donoso, M.M. Silva, Ionically conducting Er3+-doped DNA-based biomembranes forelectrochromic devices, Electrochim. Acta 120 (2014) 327.
[21] R. Leones, M. Fernandes, R.A.S. Ferreira, I. Cesarino, J.F. Lima, L.D. Carlos, V.d.Z. Bermudez, C.J. Magon, J.P. Donoso, M.M. Silva, A. Pawlicka, Luminescent DNA- and agar-based membranes, J. Nanosci. Nanotechnol. 14 (2014) 6685.
[22] L.M.N. Assis, J.R. Andrade, L.H.E. Santos, A.J. Motheo, B. Hajduk, M. Łapkowski, A. Pawlicka, Spectroscopic and microscopic study of Prussian blue film for electrochromic device application, Electrochim. Acta 4781 (2015) 176.
[23] L.M.N. Assis, L. Ponez, A. Januszko, K. Grudzinski, A. Pawlicka, A green-yellow reflective electrochromic device, Electrochim. Acta 111 (2013) 299.
[24] K. Itaya, T. Ataka, S. Toshima, Spectroelectrochemistry and electrochemical preparation method of Prussian blue modified electrodes, J. Am. Chem. Soc. 104 (1982) 4767.
[25] A. Roig, J. Navarro, J.J. Garcia, F. Vicente, Voltammetric study on the stability of deposited Prussian blue films against successive potential cycling, Electrochim. Acta 39 (1994) 437.
[26] M. Fernandes, S.S. Nobre, L.C. Rodrigues, A. Goncalves, R. Rego, M.C. Oliveira, R.A.S. Ferreira, E. Fortunato, M.M. Silva, L.D. Carlos, V.D. Bermudez, Li+- and Eu3+-doped poly(epsilon-caprolactone)/siloxane biohybrid electrolytes for electrochromic devices, ACS Appl. Mater. Interfaces 3 (2011) 2953.
[27] F. Sentanin, Desenvolvimento de janelas eletrocrômicas, Escola de Engenharia de São Carlos, Instituto de Física de São Carlos e Instituto de Química de São Carlos, Universidade de São Paulo, Sao Carlos, 2012.
[28] R.G. Zgârian, G.T. Tihan, F. Kajzar, I. Rău, A. Pawlicka, M.V. Mîndroiu, Chromophore doped DNA based solid polymer electrolyte for electrochromic devices, Arab. J. Chem. (2015), http://dx.doi.org/10.1016/j.arabjc.2015.08.007.

[29] R.J. Mortimer, D.R. Rosseinsky, Electrochemical polychromicity in iron hexacyanoferrate films, and a new film form of ferric ferricyanide, J. Electroanal. Chem. and Interfacial Electrochemistry 151 (1983) 133.
[30] C.A. Lundgren, R.W. Murray, Observations on the composition of Prussian blue films and their electrochemistry, Inorg. Chem. 27 (1988) 933.
[31] C.O. Avellaneda, D.F. Vieira, A. Al-Kahlout, S. Heusing, E.R. Leite, A. Pawlicka, M.A. Aegerter, All solid-state electrochromic devices with gelatin-based electrolyte, Sol. Energy Mater. Sol. Cells 92 (2008) 228.
[32] A. Pawlicka, J. Grote, F. Kajzar, I. Rau, M.M. Silva, Agar and DNA bio-membranes for electrochromic devices applications, Nonlin. Optics Quant. Optics 45 (2012) 113.
[33] A. Al-Kahlout, D. Vieira, C.O. Avellaneda, E.R. Leite, M.A. Aegerter, A. Pawlicka, Gelatin-based protonic electrolyte for electrochromic windows, Ionics 16 (2010) 13.
[34] R. Leones, F. Sentanin, L.C. Rodrigues, I.M. Marrucho, J.M.S.S. Esperança, A. Pawlicka, M.M. Silva, Investigation of polymer electrolytes based on agar and ionic liquids, Express Polym Lett 6 (2012) 1007.
[35] R.G.F. Costa, C.O. Avellaneda, A. Pawlicka, S. Heusing, M.A. Aegerter, Optoelectrochemical characterization of electrochromic devices with starch based solid electrolytes, Mol. Cryst. Liq. Cryst. 447 (2006) 363.
[36] D. Giménez-Romero, P.R. Bueno, J.J. García-Jareño, C. Gabrielli, H. Perrot, F. Vicente, Mechanism for interplay between electron and ionic fluxes in KhFek[Fe(CN)6]l ,mH2O compounds, J. Phys. Chem. B 110 (2006) 2715.
[37] J. Agrisuelas, J.J. García-Jareño, C. Moreno-Guerrero, A. Roig, F. Vicente, Identification of electroactive sites in Prussian Yellow films, Electrochim. Acta 113 (2013) 825.
[38] The mirror as a module, http://www.gentex.com/automotive/mirror-module (accessed on 11/06/2015).
[39] Electrochromic windows, http://www.commercialwindows.org/electrochromic.php (accessed on 23/03/2015).
[40] J. Padilla, V. Seshadri, J. Filloramo, W.K. Mino, S.P. Mishra, B. Radmard, A. Kumar, G.A. Sotzing, T.F. Otero, High contrast solid-state electrochromic devices from substituted 3, 4-propylenedioxythiophenes using the dual conjugated polymer approach, Synth. Met. 157 (2007) 261.
[41] L. Fernandes, E. Lee, G. Ward, Lighting energy savings potential of split-pane electrochromic windows controlled for daylighting with visual comfort, Energy and Buildings 61 (2013) 8.